Interaction-generated frustration in the ferromagnetic spin system on the kagome lattice: Exact analysis on the star kagomelike recursive lattice

E. Jurčišinová and M. Jurčišin
Institute of Experimental Physics, Slovak Academy of Sciences, Watsonova 47, 040 01 Košice, Slovakia

(Received 4 August 2021; accepted 7 October 2021; published 19 October 2021)

Frustration effects caused by the presence of the six-site interaction in the ferromagnetic spin-1/2 Ising system on the kagome lattice are investigated in detail using the star kagomelike recursive lattice approximation. It is shown that although the model always exhibits the existence of only two standard phases (the ferromagnetic phase and the paramagnetic one) separated by the curve of the second-order phase transitions, depending on the value of the multisite interaction, the ferromagnetic phase splits into three different ground states in the zero-temperature limit with different magnetization and thermodynamic properties. The free energy of the model is derived, the residual entropies of all ground states are determined, and it is shown that the presence of the six-site multisite interaction leads to the formation of two highly macroscopically degenerated ground states in the studied ferromagnetic system, one of which is realized only for unique ratio of the six-site interaction to the ferromagnetic interaction. It is demonstrated that the existence of this highly macroscopically degenerated single-point-like ground state leads to appearance of the Schottky anomaly in the low-temperature behavior of the specific heat capacity in the vicinity of this ground state. It is also shown that the simultaneous presence of the frustration and of the second-order phase transitions in the studied model is responsible for the existence of even three local maxima in the temperature behavior of the specific heat capacity.

DOI: 10.1103/PhysRevE.104.044121

I. INTRODUCTION

Among the most intensively experimentally as well as theoretically studied phenomena in the framework of condensed matter physics for a long time now belongs the phenomenon of frustration in various magnetic systems (see, e.g., Refs. [1–7] and references cited therein). This unquenchable interest is given by the existence of various peculiar magnetic and thermodynamic properties of such magnetic systems, among which the most interesting are the formation of different discrete systems of highly macroscopically degenerated ground states or the existence of the anomalous low-temperature behavior of the specific heat capacity that leads, e.g., to huge magnetocaloric effects. Moreover, these special properties of frustrated magnetic systems are interesting not only from pure fundamental point of view but can also have nontrivial applications, e.g., in adiabatic (de)magnetization cooling processes (see, e.g., Refs. [8–16] as well as references cited therein).

The phenomenon of the magnetic frustration is usually associated with the antiferromagnetic systems on regular lattices with elementary cycles formed by odd number of sites (most frequently formed by three sites), i.e., for instance, on the kagome, triangular, pyrochlore, or Shastry-Sutherland lattice [17]. However, more than 20 years ago the existence of geometric frustration in a ferromagnetic system was observed for the first time that was generated by the single-ion anisotropy in the ferromagnetic pyrochlore $Ho_2Ti_2O_7$ [18], which are known as the spin-ice systems (see, e.g., Refs. [18–20]). Another possibility how to obtain strong frustration in ferromagnetic systems (even on bipartite lattices) is inclusion of additional antiferromagnetic interactions (see, e.g., Refs. [21,22]). This is, however, quite expected situation since, e.g., the presence of a strong enough next-nearest-neighbor antiferromagnetic interaction can naturally caused geometric frustration in the nearest-neighbor ferromagnetic system even on the square or cubic lattices.

On the other hand, it was shown quite recently that nontrivial frustration effects can also be generated by the presence of a multisite interaction in the pure ferromagnetic system [23]. There the systematic investigation of the influence of the multisite interaction among three spin variables of each elementary triangle of the kagome lattice on the properties of the ferromagnetic system was performed in the framework of the exactly solvable model on the kagomelike Husimi lattice, i.e., on the recursive lattice that takes into account basic triangular structure of the regular kagome lattice (see, e.g., Refs. [24–33] and references cited therein). However, it was also shown that, in such a system, the frustration appears only when strong-enough external magnetic field is applied. On the other hand, in zero external magnetic field, regardless of the strength and sign of the multisite interaction, the system behaves as a ferromagnetic system. Thus, it turns out that the presence of only the interaction of this kind is not enough to cause frustration in the ferromagnetic system on the kagome lattice when magnetic field is not applied. Therefore, the open question is whether there exists another nontrivial interaction on the kagome lattice (except a pure antiferromagnetic one) that could cause frustration in the ferromagnetic system even without the presence of the external magnetic field, i.e., without the help of the explicit symmetry breaking caused by the magnetic field.

As we shall see in the present paper, such a nontrivial interaction really exists, namely the six-site interaction among all sites of each elementary hexagon of the kagome lattice. Thus, in what follows, we intend to investigate in detail the magnetic and thermodynamic properties of the ferromagnetic system on the kagome lattice with the presence of the aforementioned six-site interaction in the framework of the spin-1/2 ferromagnetic Ising model on the star kagomelike recursive lattice that takes into account not only the basic triangular structure and the coordination number of the real two-dimensional kagome lattice but also its typical starlike structure [34]. Let us note that the star kagomelike recursive lattice approximation is the simplest recursive lattice approximation of the regular kagome lattice that allows one to consider systematically the presence of this six-site interaction. As will be shown, the presence of the six-site interaction in the model leads to the frustration effects (e.g., the formation of nontrivial system of macroscopically degenerated ground states or the existence of anomalies in the low-temperature behavior of the specific heat capacity) even without the presence of the external magnetic field. This is a nontrivial fact that, on the one hand, demonstrates serious qualitative differences between various multisite interactions and, on the other hand, allows one potentially to use such kind of interactions for the explanation of properties of some frustrated magnetic systems, which exhibit simultaneously ferromagnetic and typical frustrated properties.

Last, let us note that the studied model is also interesting from pure theoretical point of view since is exactly solvable and therefore enlarges rather restricted set of exactly solvable models of the statistical mechanics. Moreover, it also enlarges the spectrum of nontrivial results obtained in the framework of investigations of various magnetic systems on the kagome and kagomelike lattices (see, e.g., Refs. [35–41] and references cited therein).

The paper is organized as follows. In Sec. II, the model is defined and formulated in the form of the recursion relations. In Sec. III, the phase diagram of the model is investigated in detail. In Sec. IV, the magnetization and entropy properties of the model are studied and the system of all ground states is found and described. The specific heat capacity and its low-temperature anomalies are studied in Sec. V. In Sec. VI, the main results of the paper are briefly summarized.

II. SPIN-1/2 FERROMAGNETIC ISING MODEL ON THE STAR KAGOMELIKE RECURSIVE LATTICE WITH SIX-SITE INTERACTION

Thus, in what follows, our aim is to analyze the properties of the ferromagnetic spin-1/2 Ising model on the kagome lattice with the presence of the six-site interaction among all sites of each elementary hexagon in the framework of the star kagomelike recursive lattice approximation. It means that the model will be studied on the recursive lattice shown explicitly in Fig. 1, which represents a higher recursive lattice approximation of the regular two-dimensional kagome lattice (see also Ref. [34] for more details).

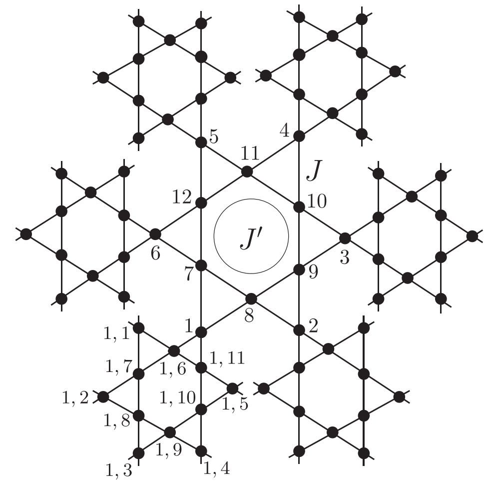

FIG. 1. The geometrical structure of the star kagomelike recursive lattice. J denotes the nearest-neighbor interaction and J' in the circle denotes the six-site interaction among all sites of each elementary hexagon of the lattice. The 12 sites of the central star of the considered recursive lattice as well as the sites of one star of the next layer of the lattice are numbered explicitly for better understanding of the derivation of the recursive relations of the model given in the Appendix.

The Hamiltonian of the model is given as follows:

$$\mathcal{H} = -J \sum_{\langle i\, j\rangle} s_i s_j - J' \sum_{\langle i_1 \ldots i_6\rangle} \prod_{j=1}^{6} s_{i_j}, \tag{1}$$

where all spin variables s_i acquire two possible values ± 1, $J > 0$ is the nearest-neighbor ferromagnetic interaction parameter and J' represents the interaction between six sites of each elementary hexagon of the lattice (see Fig. 1). The first sum in Eq. (1) runs over all nearest-neighbor spin pairs and the second sum runs over all elementary hexagons of the recursive lattice.

In the framework of the recursive lattice analysis of the studied magnetic system all physical properties of the model are driven by the stable fixed points of the corresponding recursive relations (see, e.g., Ref. [42] for all general technical details of the recursive lattice technique). The studied model is completely described by the stable fixed points $x = \lim_{n\to\infty} x_n$ of the following single recursion relation:

$$x_n = Y_1/Y_2, \tag{2}$$

where

$$\begin{aligned} Y_1 = {} & x_{n-1}^5(8e^{-6K-K'} + 12e^{-2K-K'} + 6e^{2K-K'} + 6e^{10K-K'} + 10e^{K'-6K} + 6e^{K'-2K} + 9e^{2K+K'} + 6e^{6K+K'} \\ & + e^{18K+K'}) + x_{n-1}^4(30e^{-6K-K'} + 70e^{-2K-K'} + 20e^{2K-K'} + 30e^{6K-K'} + 10e^{10K-K'} + 35e^{K'-6K} \\ & + 45e^{K'-2K} + 60e^{2K+K'} + 10e^{6K+K'} + 5e^{10K+K'} + 5e^{14K+K'}) + x_{n-1}^3(60e^{-6K-K'} + 104e^{-2K-K'} \end{aligned}$$

$$+100e^{2K-K'}+48e^{6K-K'}+8e^{10K-K'}+50e^{K'-6K}+124e^{K'-2K}+100e^{2K+K'}+28e^{6K+K'}+18e^{10K+K'})$$
$$+x_{n-1}^2(62e^{-6K-K'}+84e^{-2K-K'}+132e^{2K-K'}+36e^{6K-K'}+6e^{10K-K'}+42e^{K'-6K}+144e^{K'-2K}$$
$$+72e^{2K+K'}+56e^{6K+K'}+6e^{10K+K'})+x_{n-1}(30e^{-6K-K'}+52e^{-2K-K'}+50e^{2K-K'}+24e^{6K-K'}+4e^{10K-K'}$$
$$+25e^{K'-6K}+62e^{K'-2K}+50e^{2K+K'}+14e^{6K+K'}+9e^{10K+K'})+6e^{-6K-K'}+14e^{-2K-K'}+4e^{2K-K'}$$
$$+6e^{6K-K'}+2e^{10K-K'}+7e^{K'-6K}+9e^{K'-2K}+12e^{2K+K'}+2e^{6K+K'}+e^{10K+K'}+e^{14K+K'} \quad (3)$$

and

$$Y_2=x_{n-1}^5(6e^{-6K-K'}+14e^{-2K-K'}+4e^{2K-K'}+6e^{6K-K'}+2e^{10K-K'}+7e^{K'-6K}+9e^{K'-2K}+12e^{2K+K'}$$
$$+2e^{6K+K'}+e^{10K+K'}+e^{14K+K'})+x_{n-1}^4(30e^{-6K-K'}+52e^{-2K-K'}+50e^{2K-K'}+24e^{6K-K'}+4e^{10K-K'}$$
$$+25e^{K'-6K}+62e^{K'-2K}+50e^{2K+K'}+14e^{6K+K'}+9e^{10K+K'})+x_{n-1}^3(62e^{-6K-K'}+84e^{-2K-K'}+132e^{2K-K'}$$
$$+36e^{6K-K'}+6e^{10K-K'}+42e^{K'-6K}+144e^{K'-2K}+72e^{2K+K'}+56e^{6K+K'}+6e^{10K+K'})+x_{n-1}^2(60e^{-6K-K'}$$
$$+104e^{-2K-K'}+100e^{2K-K'}+48e^{6K-K'}+8e^{10K-K'}+50e^{K'-6K}+124e^{K'-2K}+100e^{2K+K'}+28e^{6K+K'}$$
$$+18e^{10K+K'})+x_{n-1}(30e^{-6K-K'}+70e^{-2K-K'}+20e^{2K-K'}+30e^{6K-K'}+10e^{10K-K'}+35e^{K'-6K}$$
$$+45e^{K'-2K}+60e^{2K+K'}+10e^{6K+K'}+5e^{10K+K'}+5e^{14K+K'})+8e^{-6K-K'}+12e^{-2K-K'}+6e^{2K-K'}$$
$$+6e^{10K-K'}+10e^{K'-6K}+6e^{K'-2K}+9e^{2K+K'}+6e^{6K+K'}+e^{18K+K'}, \quad (4)$$

and where $K=J/(k_BT)$, $K'=J'/(k_BT)$, T is the temperature, and k_B is the Boltzmann constant. The detailed derivation of the recursion relation (2) is given in the Appendix.

In general, when more than one physically acceptable stable fixed points of the recursion relation (2) exist then, to be able to decide which of them describes thermodynamically stable phase of the model, the knowledge of the free energy per site of the model is needed. Even if there is only one stable fixed point of the recursion relation, the knowledge of the free energy is needed for a detailed analysis of the thermodynamic properties of the model. In this respect, the free energy per site f of the studied model on the star kagomelike recursive lattice can be derived, e.g., using the techniques described in Refs. [43,44] and has the following form:

$$\beta f=\frac{1}{9}\ln\frac{F_1^2}{F_2^3}, \quad (5)$$

where $\beta=1/(k_BT)$ and

$$F_1=e^{-6K-K'}[(x^6+1)e^{24K+2K'}+6x(x^4+1)e^{20K+2K'}+36e^{12K}x(x^2+1)(x+1)^2+6e^{16K}(x^4+x^2+1)(x+1)^2$$
$$+3x(2x^4+9x^3+4x^2+9x+2)e^{2(8K+K')}+6e^{8K}(x^4+2x^3+20x^2+2x+1)(x+1)^2$$
$$+12e^{4K}(x^4+5x^3+2x^2+5x+1)(x+1)^2+6(x^6+9x^5+31x^4+48x^3+31x^2+9x+1)e^{4K+2K'}$$
$$+2(3x^6+6x^5+21x^4+56x^3+21x^2+6x+3)e^{2(6K+K')}+3(3x^6+24x^5+50x^4+48x^3+50x^2+24x+3)e^{8K+2K'}$$
$$+2(4x^4+10x^3+21x^2+10x+4)(x+1)^2+(10x^6+42x^5+75x^4+84x^3+75x^2+42x+10)e^{2K'}], \quad (6)$$

$$F_2=e^{-6K-K'}[(x^4+5)xe^{20K+2K'}+(x^4+9x^3+6x^2+18x+5)xe^{2(8K+K')}+6e^{12K}(x^4+4x^3+6x^2+8x+5)x$$
$$+2(x^5+7x^4+28x^3+14x^2+5x+3)e^{2(6K+K')}+(9x^5+62x^4+144x^3+124x^2+45x+6)e^{4K+2K'}$$
$$+(12x^5+50x^4+72x^3+100x^2+60x+9)e^{8K+2K'}+2e^{16K}(x^5+2x^4+3x^3+4x^2+5x+3)$$
$$+2e^{8K}(2x^5+25x^4+66x^3+50x^2+10x+3)+2e^{4K}(7x^5+26x^4+42x^3+52x^2+35x+6)$$
$$+e^{24K+2K'}+6x^5+30x^4+62x^3+60x^2+30x+8+(7x^5+25x^4+42x^3+50x^2+35x+10)e^{2K'}], \quad (7)$$

and x represents the corresponding stable fixed point of the recursion relation (2).

To conclude this section, let us note that, having the explicit expression for the free energy of the model as the function of the model parameters as well as of the fixed point value x, the present model represents an exactly solvable model, what will be demonstrated in the subsequent sections.

III. THE PHASE DIAGRAM OF THE MODEL

Before we investigate the influence of the six-site interaction on the phase transitions of the model, let us first determine and discuss the value of the critical temperature of the pure ferromagnetic system ($J'=0$) on the star kagomelike recursive lattice and compare it to the corresponding values of the critical temperature obtained in the framework of two simpler recursive lattice approximations, i.e., in the framework of the Bethe lattice approximation with $k_BT_c/J \approx 2.8856$ [42] and in the framework of the Husimi lattice approximation with $k_BT_c/J \approx 2.4852$ [45], as well as to its exact value $k_BT_c/J \approx 2.1432$ for the Ising model on the regular kagome lattice [46].

First, it is clear that the Husimi recursive lattice approximation of the model, which takes into account more information about the geometrical structure of the regular kagome lattice in comparison to the Bethe lattice approximation, gives also far better approximative value for the critical temperature. Therefore, it can be expected that the critical temperature of the model on the star kagomelike recursive lattice will again be closer to its exact value on the regular kagome lattice. The open question is how significant is this correction.

The critical temperature of the spin-1/2 ferromagnetic Ising model on the star kagomelike recursive lattice is given by the unique real positive solution y_c of the following polynomial equation of the six order:

$$-76 - 187y - 171y^2 - 70y^3 - 10y^4 + y^5 + y^6 = 0, \quad (8)$$

with

$$\frac{k_BT_c}{J} = \frac{4}{\ln y_c} \approx 2.4431. \quad (9)$$

This result shows that transition from the Husimi lattice approximation to the star kagomelike recursive lattice approximation of the model on the kagome lattice slightly improves the value of the critical temperature.

However, as was discussed in the Introduction, the main advantage of the star kagomelike recursive lattice approximation of the model is the possibility to include further interactions and study their influence on the model properties.

In this respect, the analysis shows that the presence of the six-site interaction in the model preserves the existence of the second-order phase transitions between the ferromagnetic phase and the paramagnetic one, regardless of its strength and sign. The corresponding phase diagram in the $\alpha = J'/J$ versus k_BT/J plane is shown in Fig. 2. At the same time, the curve of the critical temperatures in Fig. 2 is given by the following equation:

$$\begin{aligned}&- 47 - 29e^{2\alpha K_c} - 119e^{2(\alpha+2)K_c} - 65e^{2(\alpha+4)K_c}\\ &- 34e^{2(\alpha+6)K_c} - 11e^{2(\alpha+8)K_c} + e^{2(\alpha+10)K_c} + e^{2(\alpha+12)K_c}\\ &- 68e^{4K_c} - 106e^{8K_c} - 36e^{12K_c} + e^{16K_c} = 0, \end{aligned} \quad (10)$$

where $k_BT_c/J = K_c^{-1}$ can be calculated for given value of the parameter $\alpha \in (-\infty, \infty)$.

Note also that Eq. (10) can be solved with respect to α. Thus, it is possible to determine directly the critical value α_c of the parameter α for given value of the reduced critical temperature K_c^{-1}, namely

$$\alpha_c = \frac{1}{2K_c} \ln \frac{A}{B}, \quad (11)$$

where

$$A = 47 + 68e^{4K_c} + 106e^{8K_c} + 36e^{12K_c} - e^{16K_c} \quad (12)$$

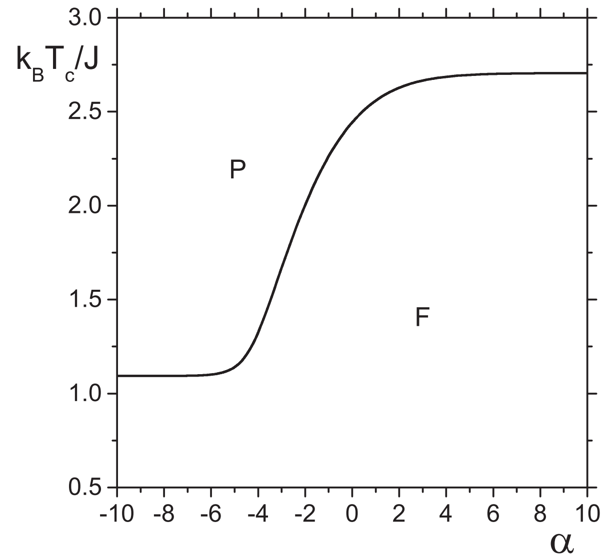

FIG. 2. The phase diagram of the model in the $\alpha = J'/J$ versus k_BT/J plane in the star kagomelike recursive lattice approximation. The curve represents the reduced critical temperatures k_BT_c/J of the second-order phase transitions of the model between the ferromagnetic phase (F) and the paramagnetic phase (P).

and

$$\begin{aligned}B =& - 29 - 119e^{4K_c} - 65e^{8K_c} - 34e^{12K_c} - 11e^{16K_c}\\ &+ e^{20K_c} + e^{24K_c}\end{aligned} \quad (13)$$

Here the values of the critical temperatures K_c^{-1} are restricted to the interval $1.0935 < K_c^{-1} < 2.7057$ (see Fig. 2), where the lower value is given by the real positive solution of the following equation:

$$A = 0. \quad (14)$$

Since this equation is a polynomial equation of the fourth order with respect to e^{4K_c}, the explicit analytic expression for the critical temperature in the limit $\alpha \to -\infty$ exists, namely

$$\left.\frac{k_BT_c}{J}\right|_{\alpha\to-\infty} = \frac{4}{\ln y} \approx 1.0935, \quad (15)$$

where

$$y = 9 + \frac{2}{b} + \frac{1}{2}\sqrt{\frac{16}{3}\left(148 + \frac{13}{a} + a\right) + 3904b} \quad (16)$$

and

$$b = \sqrt{\frac{3}{74 - 13/a - a}}, \quad a = (235 - 6\sqrt{1473})^{1/3}. \quad (17)$$

On the other hand, the upper bound of the critical temperatures is defined as the corresponding real positive solution of the equation

$$B = 0. \quad (18)$$

As follows from Fig. 2, the presence of the six-site interaction in the model with the positive sign of the parameter J' leads to the increasing of the value of the critical temperature of the pure ferromagnetic model. At the same time, the corresponding dependence is relatively weak. On the other hand, significantly stronger dependence of the critical temperature on the strength of the six-site interaction is observed for its negative sign. In this case, the presence of the six-site interaction strongly reduces the value of the critical temperature especially for its relatively small absolute values in comparison to the nearest-neighbor ferromagnetic interaction. However, it is also worth mentioning that, regardless of the sign of the six-site interaction, the position of the critical temperatures of the model very slightly depend on its strength already for not very large absolute values of the parameter α.

Thus, at the first sight, it seems that the presence of the six-site interaction in the spin-1/2 ferromagnetic Ising model on the kagome lattice has only quantitative impact on the critical behavior but nothing is changed qualitatively. However, as we shall see in the next section, the six-site interaction has nontrivial impact on the low-temperature thermodynamics of the model. Its presence introduces the frustration into the pure ferromagnetic system for negative values of the parameter α with the appearance of a well-defined system of highly macroscopically degenerated ground states.

IV. MAGNETIZATION AND ENTROPY OF THE MODEL: GROUND-STATE ANALYSIS AND RESIDUAL ENTROPIES

First, let us analyze in detail the behavior of the magnetization and entropy of the model. The magnetization of the studied model on the star kagomelike recursive lattice can be derived in the standard way [42] and has the following form:

$$m = \frac{1}{3}\frac{M_1}{M_2}, \tag{19}$$

where

$$\begin{aligned} M_1 = {} & x^6(2e^{4K+2K'} + 15e^{8K+2K'} + 10e^{12K+2K'} + 3e^{24K+2K'} + 12e^{4K} + 6e^{8K} + 14e^{16K} + 2e^{2K'}) + x^5(16e^{4K+2K'} \\ & + 72e^{8K+2K'} + 16e^{12K+2K'} + 8e^{16K+2K'} + 16e^{20K+2K'} + 24e^{4K} + 16e^{8K} + 56e^{12K} + 24e^{16K} + 8) \\ & + x^4(58e^{4K+2K'} + 50e^{8K+2K'} + 18e^{12K+2K'} + 47e^{16K+2K'} - 12e^{4K} + 50e^{8K} + 88e^{12K} + 12e^{16K} - 13e^{2K'} + 22) \\ & + x^2(-58e^{4K+2K'} - 50e^{8K+2K'} - 18e^{12K+2K'} - 47e^{16K+2K'} + 12e^{4K} - 50e^{8K} - 88e^{12K} - 12e^{16K} + 13e^{2K'} \\ & - 22) + x(-16e^{4K+2K'} - 72e^{8K+2K'} - 16e^{12K+2K'} - 8e^{16K+2K'} - 16e^{20K+2K'} - 24e^{4K} - 16e^{8K} - 56e^{12K} \\ & - 24e^{16K} - 8) - 2e^{4K+2K'} - 15e^{8K+2K'} - 10e^{12K+2K'} - 3e^{24K+2K'} - 12e^{4K} - 6e^{8K} - 14e^{16K} - 2e^{2K'} \end{aligned} \tag{20}$$

and

$$\begin{aligned} M_2 = {} & x^6(6e^{4K+2K'} + 9e^{8K+2K'} + 6e^{12K+2K'} + e^{24K+2K'} + 12e^{4K} + 6e^{8K} + 6e^{16K} + 10e^{2K'} + 8) + x^5(54e^{4K+2K'} \\ & + 72e^{8K+2K'} + 12e^{12K+2K'} + 6e^{16K+2K'} + 6e^{20K+2K'} + 84e^{4K} + 24e^{8K} + 36e^{12K} + 12e^{16K} + 42e^{2K'} + 36) \\ & + x^4(186e^{4K+2K'} + 150e^{8K+2K'} + 42e^{12K+2K'} + 27e^{16K+2K'} + 156e^{4K} + 150e^{8K} + 72e^{12K} + 12e^{16K} + 75e^{2K'} \\ & + 90) + x^3(288e^{4K+2K'} + 144e^{8K+2K'} + 112e^{12K+2K'} + 12e^{16K+2K'} + 168e^{4K} + 264e^{8K} + 72e^{12K} + 12e^{16K} \\ & + 84e^{2K'} + 124) + x^2(186e^{4K+2K'} + 150e^{8K+2K'} + 42e^{12K+2K'} + 27e^{16K+2K'} + 156e^{4K} + 150e^{8K} + 72e^{12K} \\ & + 12e^{16K} + 75e^{2K'} + 90) + x(54e^{4K+2K'} + 72e^{8K+2K'} + 12e^{12K+2K'} + 6e^{16K+2K'} + 6e^{20K+2K'} + 84e^{4K} \\ & + 24e^{8K} + 36e^{12K} + 12e^{16K} + 42e^{2K'} + 36) + 6e^{4K+2K'} + 9e^{8K+2K'} + 6e^{12K+2K'} + e^{24K+2K'} + 12e^{4K} + 6e^{8K} \\ & + 6e^{16K} + 10e^{2K'} - 8. \end{aligned} \tag{21}$$

On the other hand, the entropy per site s of the model can be calculated directly from the free energy per site of the model (5) using the well-known definition $s = -\partial f/\partial T$.

The temperature dependence of the magnetization of the model for various values of the parameter α is shown explicitly in Fig. 3. As follows from this figure, the model exhibits the existence of the spontaneous magnetization below the corresponding values of the critical temperatures with formation of three different ground states with well-defined magnetization values in the zero-temperature limit. Moreover, the spontaneous magnetization is realized in the restricted area bounded by the corresponding magnetization curves obtained in the limits $\alpha \to \infty$ [the upper dashed (red) curve in Fig. 3] and $\alpha \to -\infty$ [the lower dashed (red) curve in Fig. 3].

The formation of three different ground states of the model indicates that the six-site interaction for the negative values of the interaction parameter J' generates in fact nontrivial frustration in the studied ferromagnetic system. The presence of the frustration is also clearly visible in the entropy behavior of the model since two of three model ground states exhibit nonzero residual entropies, i.e., they are highly macroscopically degenerated. This is explicitly demonstrated in Figs. 4 and 5, where the dependence of the magnetization (Fig. 4) and the entropy (Fig. 5) on the parameter α is shown for various values of the reduced temperature. At the same time, the magnetization and entropy properties of three ground states of the model are also demonstrated in the corresponding bottom figures in Figs. 4 and 5.

Thus, as follows from Figs. 4 and 5, the model exhibits the existence of two plateaulike ground states, which are realized for $\alpha > -4$ and $\alpha < -4$, respectively. One of them ($\alpha > -4$) represents the standard ferromagnetic ground state

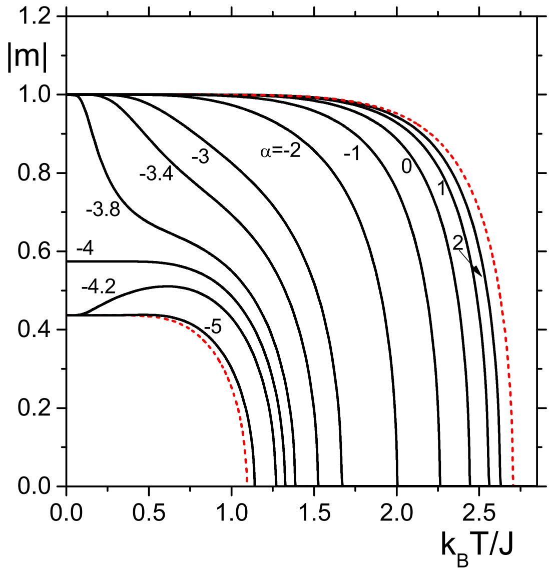

FIG. 3. The absolute value of the spontaneous magnetization of the model as the function of the reduced temperature for various values of the parameter α. The formation of three different ground states is visible. The dashed (red) curves correspond to the spontaneous magnetizations obtained in the limits $\alpha \to \infty$ (the upper bound) and $\alpha \to -\infty$ (the lower bound).

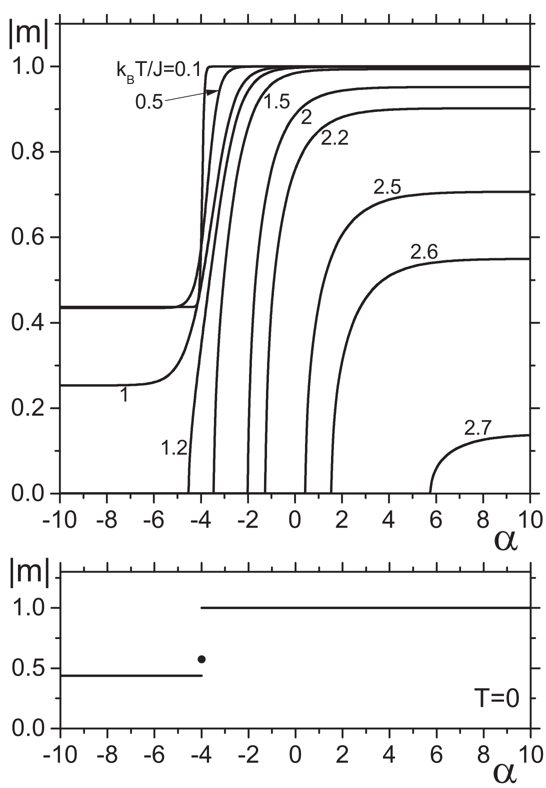

FIG. 4. The absolute value of the magnetization of the model as the function of the parameter α for various values of the reduced temperature with the explicit formation of three different ground states. The ground-state magnetizations are shown in the bottom figure.

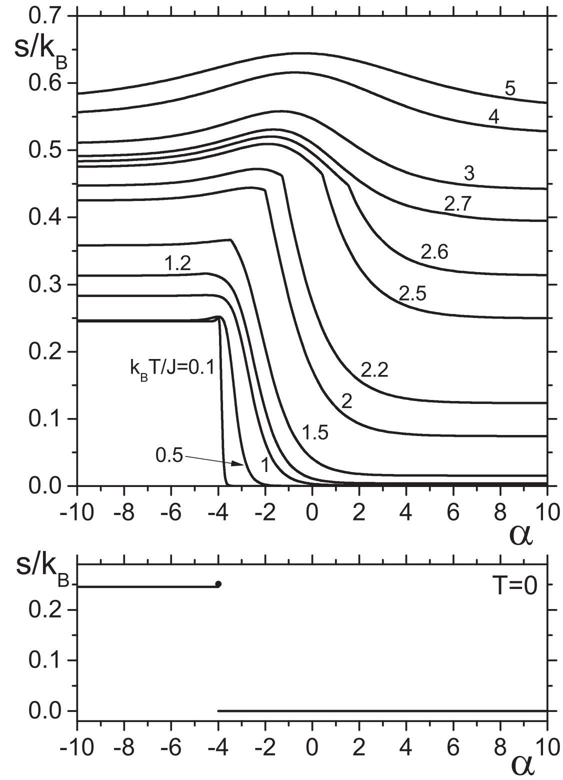

FIG. 5. The entropy per site of the model as the function of the parameter α for various values of the reduced temperatures. The residual entropies of three different ground states of the model are demonstrated in the bottom figure.

with $|m| = 1$ and $s = 0$. On the other hand, the negative six-site interaction, which is more than four times stronger than the nearest-neighbor ferromagnetic interaction, causes strong frustration and leads to the formation of highly macroscopically degenerated ground state with the absolute value of the magnetization

$$|m| = \frac{1}{9}\sqrt{\frac{98\sqrt{13} - 307}{3}} \approx 0.4367 \tag{22}$$

and with the residual entropy

$$s = \frac{k_B}{9} \ln \frac{13\sqrt{13} + 35}{9} \approx 0.2453. \tag{23}$$

These two ground states are separated by the well-defined single-point-like ground state realized at $\alpha = -4$ with the residual entropy

$$s = \frac{k_B}{9} \ln \frac{19\sqrt{57} + 87}{24} \approx 0.2513 \tag{24}$$

and with the absolute value of the magnetization

$$|m| = \frac{1}{2439}\sqrt{\frac{19(124193\sqrt{57} - 731045)}{2}} \approx 0.5744. \tag{25}$$

This ground state is most macroscopically degenerated since it has the largest value of the residual entropy and, as we shall see in the next section, its existence leads to the nontrivial thermodynamics in its vicinity.

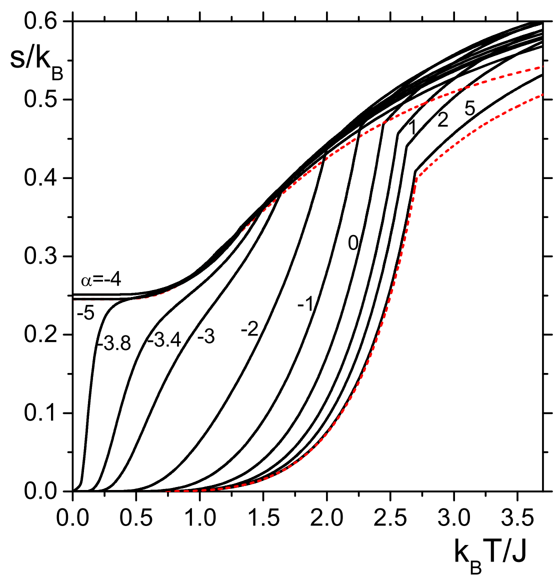

FIG. 6. The temperature dependence of the entropy per site of the model for various values of the parameter α. The dashed (red) curves corresponds to the entropies obtained in the limit $\alpha \to \infty$ (the lower dashed curve) and $\alpha \to -\infty$ (the upper dashed curve).

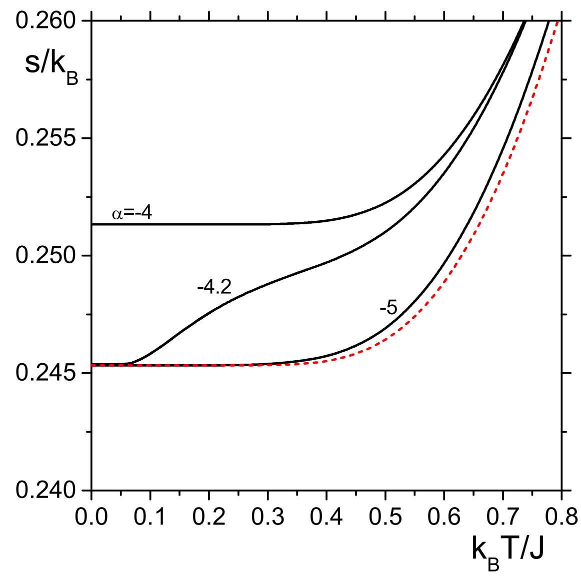

FIG. 7. The detailed figure of the formation of two different residual entropies for the single-point-like ground state at $\alpha = -4$ and for the plateaulike ground state for $\alpha < -4$. The dashed (red) curve denotes the entropy obtained in the limit $\alpha \to -\infty$.

The formation of three different ground states of the model is also clearly demonstrated in Fig. 6, where the temperature dependence of the entropy per site is shown for various values of the parameter α. Again, one can see the low-temperature behavior of the entropy with formation of hierarchy of residual entropies of the system of ground states, which is typical for frustrated magnetic systems [47,48]. At the same time, the temperature dependence of the entropy of the model approaches those given by the dashed (red) curves in the limits $\alpha \to \infty$ (the lower dashed curve) and $\alpha \to -\infty$ (the upper dashed curve). For clarity, the formation of the residual entropies of two degenerated ground states of the model is shown in detail once more in Fig. 7 since the difference between these residual entropies is very small [see Eqs. (23) and (24)].

On the other hand, the second-order character of the phase transitions is also clearly visible from the continuous behavior of the entropy at the critical temperatures (see Figs. 5 and 6). The behavior of the entropy on the curve of the critical points is explicitly shown in Fig. 8. As follows from this figure, the critical entropy obtains its maximum values in the vicinity of $\alpha = 0$. At the same time, the negative values of the parameter α reduce the value of the entropy together with the reducing of the critical temperature value. On the other hand, with the increasing of the positive values of the parameter α, the critical entropy also decreases (although not so strongly as in the case of negative values of α) but the value of the critical temperature increases.

Finally, note that the existence of the system of ground states with nonzero residual entropies in the studied model has a nontrivial impact on its thermodynamics, e.g., on the low-temperature properties of the specific heat capacity, which, as we shall see in the next section, exhibits anomalous behavior typical for the frustrated magnetic systems.

V. FRUSTRATION EFFECTS IN THE SPECIFIC HEAT CAPACITY BEHAVIOR OF THE MODEL

Having the explicit expression for the free energy per site of the model (5), the properties of the specific heat capacity c_H of the model at the constant magnetic field $H = 0$ (studied in the present paper) can be directly investigated by using the standard relations

$$c_H \equiv T\frac{\partial s}{\partial T} = -T\frac{\partial^2 f}{\partial T^2}. \tag{26}$$

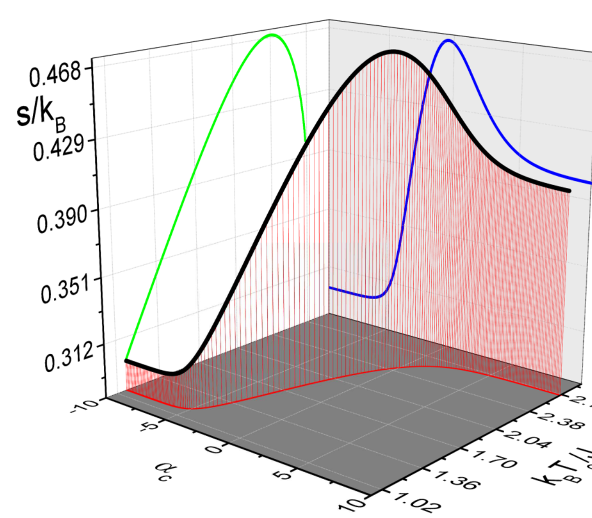

FIG. 8. The entropy per site of the model (the black curve) on the curve of the second-order phase transitions (the red curve in the plane k_BT_c/J versus α_c) together with its projections onto the planes k_BT_c/J versus s/k_B (the green curve) and α_c versus s/k_B (the blue curve).

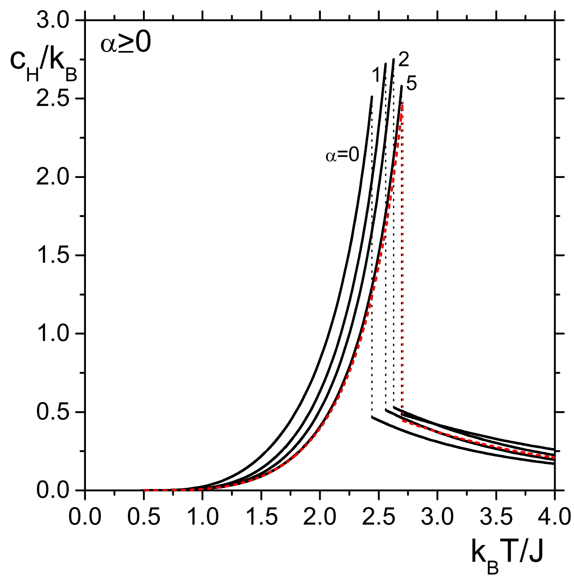

FIG. 9. The temperature dependence of the specific heat capacity for the nonnegative values of the parameter α. The dashed (red) curves correspond to the limit case $\alpha \to \infty$.

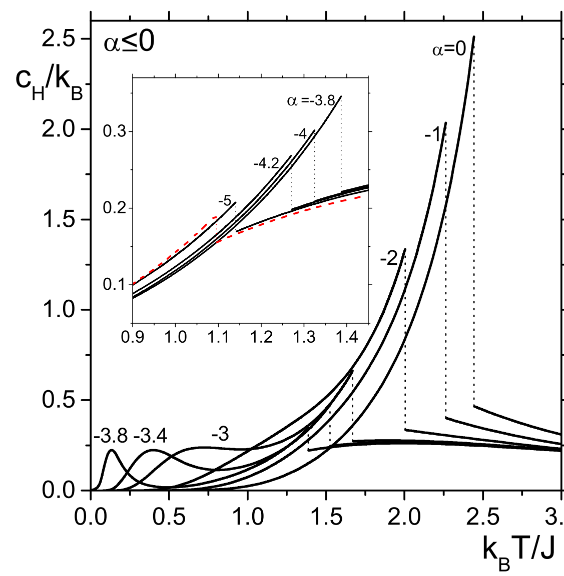

FIG. 10. The temperature dependence of the specific heat capacity for the negative values of the parameter α with explicit formation of the anomalous second peak in the low-temperature specific heat capacity behavior in the vicinity of $\alpha = -4$. The dashed (red) curves in the inset correspond to the limit case $\alpha \to -\infty$.

First, let us discuss the temperature behavior of the specific heat capacity of the model separately for various positive and negative values of the parameter α. As follows from Fig. 9, where the temperature dependence of the specific heat capacity is shown for various nonnegative values of α, the presence of the six-site interaction with positive values of J' preserves the ferromagnetic character of the basic model with very similar behavior of the specific heat capacity in the vicinity of the critical temperatures. Thus, in this case, the presence of the six-site interaction has no qualitative and only weak quantitative impact on the model thermodynamics.

On the other hand, the situation is completely different when negative six-site interaction is considered, i.e., when $\alpha < 0$. First, as follows from Fig. 10, in this case, the discontinuous jumps in the temperature behavior of the specific heat capacity at the critical temperatures are significantly reduced with the increasing of the strength of the six-site interaction with the minimal jump obtained in the limit $\alpha \to -\infty$ [see the dashed (red) curves in the detailed inset in Fig. 10]. Moreover, as can also be seen in Fig. 10, in addition to the discontinuous behavior of the specific heat capacity at the corresponding critical temperatures, the anomalous second peak appears at low temperatures for values of α from the vicinity of $\alpha = -4$, where the unique highly macroscopically degenerated single-point-like ground state is realized in the zero-temperature limit (see curves $\alpha = -3$, -3.4, and -3.8 in Fig. 10). This low-temperature behavior of the specific heat capacity is directly related to the frustration of the system represented by the presence of the residual-entropy hierarchy of three different ground states (see the previous section).

Note that, although the existence of the anomalous (Schottky) peak in the low-temperature behavior of the specific heat capacity is shown in Fig. 10 only for the right vicinity of $\alpha = -4$, i.e., for $\alpha > -4$, these frustration effects also exist in the left vicinity of $\alpha = -4$, i.e., for $\alpha < -4$. However, due to the small difference between the residual entropies of the single-point-like ground state at $\alpha = -4$ and the plateaulike ground state realized for $\alpha < -4$ (see the previous section), the corresponding frustration effects in the low-temperature specific heat capacity behavior are considerably less visible as is demonstrated in Figs. 11 and 12, where the low-temperature behavior of the specific heat capacity is compared for $\alpha =$

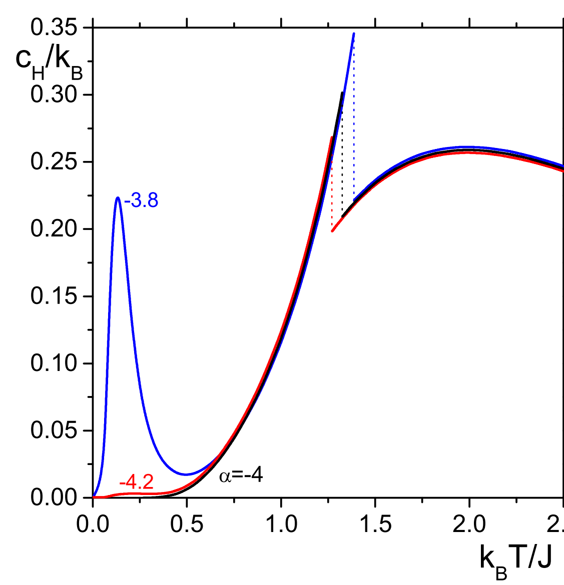

FIG. 11. The comparison of the low-temperature behavior of the specific heat capacity for $\alpha = -4$ (the black curves), for which the unique highly-macroscopically degenerated single-point-like ground state is realized in the zero-temperature limit, with the corresponding behavior of the specific heat capacity for $\alpha = -4.2$ (the red curves) and $\alpha = -3.8$ (the blue curves), i.e., for representative values from its right and left vicinity with presence of the Schottky-type anomaly.

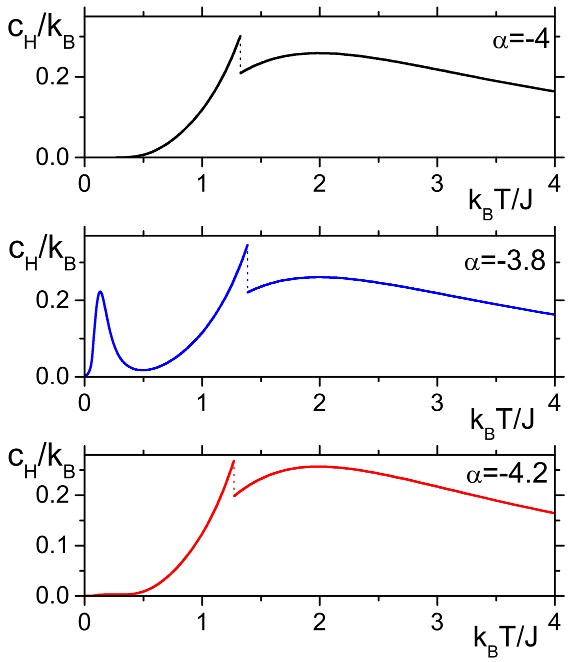

FIG. 12. The same curves of the specific heat capacity as in Fig. 11 presented separately for clarity.

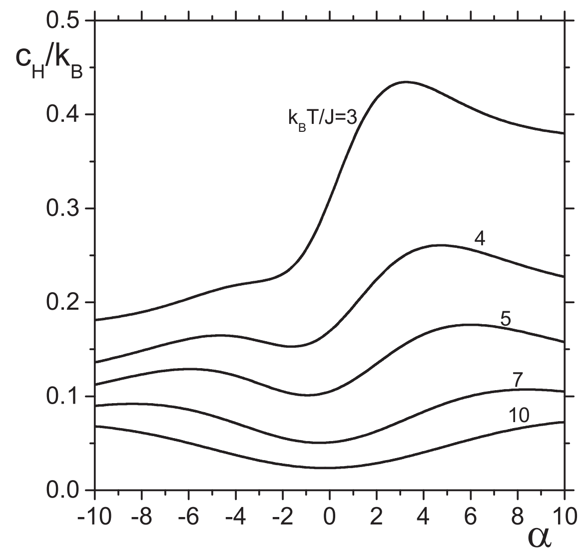

FIG. 13. The behavior of the specific heat capacity as the function of the parameter α for various values of the reduced temperatures $k_BT/J > 2.7057$, below which the second-order phase transitions appear for the corresponding values of α (see Sec. III).

-4.2, -4, and -3.8. Here it is also worth mentioning that the specific heat capacity exhibits even three maxima in its temperature dependence in the vicinity of $\alpha = -4$ (see the curves for $\alpha = -3.8$ and -4.2 in Figs. 11 and 12). In addition to the standard maximum formed at high temperatures, two other maxima are related to the simultaneous presence of the frustration effects (the formation of the Schottky peak at low temperature) and of the second-order phase transition at the corresponding critical temperature.

Finally, let us investigate in detail the behavior of the specific heat capacity as the function of the parameter α for various values of the reduced temperature. Here, depending on the temperature values, one can observed three qualitatively different situations. First, as is demonstrated in Fig. 13, the specific heat capacity behaves as a slowly changing function of α for high-enough temperatures ($k_BT/J \gg 2.7057$), i.e., for temperatures much higher than temperatures for which the second-order phase transitions exist for the corresponding values of α. On the other hand, for the reduced temperatures from the interval $1.0935 < k_BT/J < 2.7057$, for which the second-order phase transitions exist (see the discussion in Sec. II), the specific heat capacity exhibits discontinuity with finite jump at the corresponding critical value α_c of the parameter α. This behavior is explicitly shown in Fig. 14, where is also shown that the specific heat capacity again becomes the continuous function of α for $k_BT/J < 1.0935$ (see the curve for $k_BT/J = 1$ in Fig. 14). This figure also demonstrates the fact that the jump in the specific heat capacity is rapidly reduced when the temperature decreases in the interval $1.0935 < k_BT/J < 2.7057$.

In the end, the qualitatively different behavior of the specific heat capacity as the function of the parameter α appears for low-enough temperatures ($k_BT/J \ll 1$), where frustration effects take place. They lead to the formation of the typical double-peak structure in the specific heat capacity centered at $\alpha = -4$, at which the highly macroscopically degenerated single-point-like ground state is formed in the zero-temperature limit. This behavior of the specific heat capacity is demonstrated in Fig. 15. At the same time, as was discussed, e.g., in Ref. [49], the heights of the formed peaks are usually different since they are directly related to the differences between the residual entropies of the single-point-like ground state and the corresponding neighboring plateaulike ground states. This is the reason why, on the one

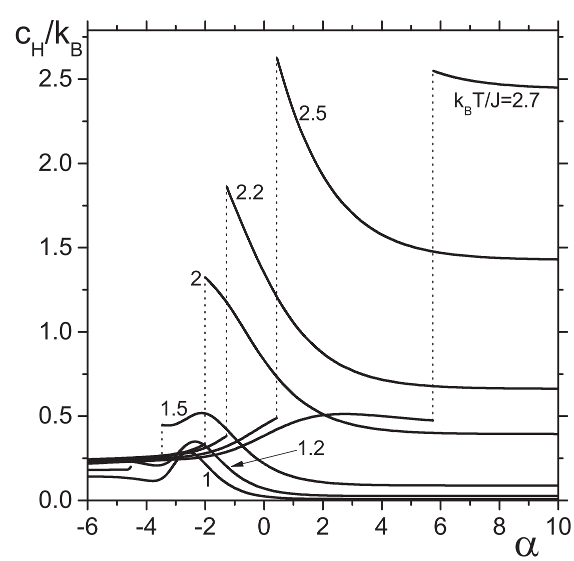

FIG. 14. The behavior of the specific heat capacity as the function of the parameter α for various values of the reduced temperatures from the interval $1.0935 < k_BT/J < 2.7057$ with discontinuous behavior at the corresponding critical points. In addition, the continuous behavior of the specific heat capacity for $k_BT/J < 1.0935$ is demonstrated by the curve $k_BT/J = 1$.

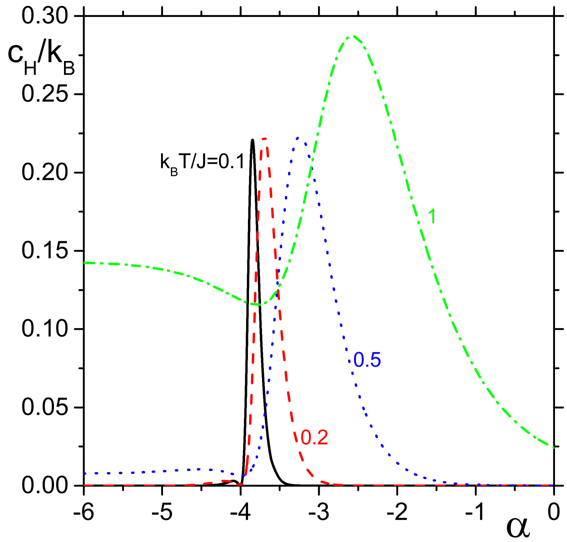

FIG. 15. The behavior of the specific heat capacity as the function of the parameter α for various values of the reduced temperatures $k_BT/J \leqslant 1$ with explicit formation of the typical double-peak structure centered at $\alpha = -4$, at which the highly macroscopically degenerated single-point-like ground state is formed in the zero-temperature limit. The fact that quite indistinct peak is form in the left vicinity of $\alpha = -4$ is related to the slight difference between the residual entropies of the neighboring ground states of the model.

hand, the formed peak in the right vicinity of $\alpha = -4$ at low temperatures is distinctive (there is significant difference between the residual entropies of the ground state formed at $\alpha = -4$ and of the ground state observed for $\alpha > -4$) and that, on the other hand, the peak formed in the left vicinity of $\alpha = -4$ is very small as a result of the fact that the difference between residual entropies of the corresponding neighboring ground states is also very small (see the previous section).

To conclude our analysis let us stress that the behavior of the specific heat capacity at low temperatures with the existence of an additional anomalous (Schottky-type) peak in its temperature dependence as well as with the formation of the typical double-peak structure in the α-dependence clearly demonstrates the frustrated character of the model caused by the presence of the six-site interaction in initially unfrustrated pure ferromagnetic system.

VI. CONCLUSION

In the end, let us summarize briefly the main results obtained in the present paper.

We have investigated in detail the influence of the presence of the six-site interaction among all sites within each elementary hexagon on the properties of the ferromagnetic spin-1/2 Ising model on the kagome lattice using the star kagomelike recursive lattice approximation. The recursion relation, fixed points of which describes possible model phases, is derived and the explicit expression for the free energy per site of the model is found. The influence of the six-site interaction on the critical temperature of the pure ferromagnetic system is analyzed. It is shown that, regardless of the strength and sign of the added six-site interaction, the model preserves its ferromagnetic character in the sense that it exhibits the existence of only two phases (the ferromagnetic and the paramagnetic) separated by the curve of the second-order phase transitions. The equation for the critical temperatures of the model as the function of the ratio α of the six-site and the nearest-neighbor interaction is found. Analysis shows that the value of the critical temperature increases with increasing of the strength of the six-site interaction for positive values of the interaction parameter J', i.e., for $\alpha > 0$. On the other hand, the increasing of the strength of the six-site interaction for J', i.e., for $\alpha < 0$, leads to the reduction of the critical temperature value, which is significantly more pronounced than its growth for positive values of J'. This behavior is related to the fact that the six-site interaction with the positive parameter J' prefers the configurations with even number of spin variables oriented in both directions, i.e., gives additional ferromagnetic effect (the increasing of the value of the critical temperature). On the other hand, the negative sign of the six-site interaction prefers the odd number of spin variables to be oriented in both direction, i.e., behaves as an interaction with antiferromagnetic effects in the geometrically frustrated system that act against the ferromagnetic character of the original system. As a result the value of the critical temperature decreases in this case. Nevertheless, the general features of the six-site interaction cause that the presence of the second-order phase transitions is preserved even in the limit $\alpha \to -\infty$, i.e., that the ferromagnetic character of the model is not completely suppressed.

However, the antiferromagnetic properties of the six-site interaction for negative values of J' completely reveal themselves at low temperatures, where the formation of two highly macroscopically degenerated ground states with well-defined magnetization and thermodynamic properties is observed. Namely, it is shown that the unique ferromagnetic phase that exists below the curve of the critical temperatures splits into three different ground states in the zero-temperature limit. One of these ground states is the standard ferromagnetic ground state with the saturated absolute value of the magnetization $|m| = 1$ and zero entropy $s = 0$ realized for $\alpha > -4$. The existence of the two additional aforementioned ground states with nontrivial values of their magnetizations and residual entropies, which are formed at $\alpha = -4$ and for $\alpha < -4$ (see Figs. 4–7), is the result of the geometric frustration caused by the presence of the six-site interaction on the kagome lattice represented here by the star kagomelike recursive lattice.

It is also shown that the existence of three different ground states in the model with the standard hierarchy of their residual entropies, i.e., the existence of the single-point-like ground state at $\alpha = -4$ with the highest macroscopic degeneration that separates two plateaulike ground states for $\alpha < -4$ and $\alpha > -4$ with smaller residual entropies, leads to the anomalous low-temperature behavior of the specific heat capacity with the appearance of the second (Schottky) peak (see Figs. 10–12), heights of which are directly related to the corresponding differences between the residual entropies of the neighboring single-point-like and plateaulike ground states. Therefore, the Schottky peak formed in the right vicinity of $\alpha = -4$ is distinctive but the Schottky peak observed in the left vicinity of $\alpha = -4$ is almost invisible (see Figs. 11 and 12).

The frustration effects caused by the presence of the six-site interaction is also demonstrated in the formation of a typical double-peak structure behavior of the specific heat capacity as the function of the parameter α at low temperatures centered at $\alpha = -4$, where the highly macroscopically degenerated single-point-like ground state is formed (see Fig. 15). Again, due to the small difference between the residual entropies of the corresponding neighboring ground states, the height of the peak formed in the left vicinity of $\alpha = -4$ is significantly suppressed.

Let us also note that the antiferromagnetic effects of the six-site interaction with negative values of J' is also visible in the discontinuous jumps of the specific heat capacity at the critical temperatures, which are significantly reduced with increasing of its strength. Moreover, the simultaneous existence of the low-temperature frustration effects and of the second-order phase transitions leads to the presence of three different local maxima in the temperature dependence of the specific heat capacity (see Figs. 11 and 12).

Finally, it is worth mentioning that similar behavior of the specific heat capacity with the presence of the Schottky peak as well as with the jump at the critical temperature was observed recently, e.g., in Ref. [50], in the framework of the antiferromagnetic material $Cs_2Cu_3CeF_{12}$ with an anisotropic kagomelike structure. There, the existence of ferromagnetic effects in antiferromagnetic systems was shown. In this respect, our analysis shows that similar thermodynamic properties can be also achieved in the ferromagnetic system on the kagome lattice with the presence of an appropriate additional interaction that simulates some additional antiferromagnetic and anisotropic properties of the system.

ACKNOWLEDGMENTS

This work was supported by the Slovak Research and Development Agency under Contract No. APVV-17-0020 as well as under Contract No. APVV-20-0293. This work was also supported by VEGA Grants No. 2/0058/19 and No. 2/0081/21 of the Slovak Academy of Sciences.

APPENDIX

In the Appendix, the derivation of the recursion relation (2) is given that drives all physical properties of the studied model. First, since the model is studied on the star kagomelike recursive lattice (see Fig. 1), the partition function of the model described by the Hamiltonian (1)

$$Z \equiv \sum_s e^{-\beta\mathcal{H}} = \sum_s e^{K\sum_{\langle ij\rangle} s_i s_j + K' \sum_{\langle i_1,\dots,i_6\rangle} \prod_{j=1}^{6} s_{i_j}}, \tag{A1}$$

can be written in the following explicit recursive form (see Fig. 1 as for numbering of the twelve sites of the central star of the studied recursive lattice):

$$Z = \sum_{s_1,\dots s_{12}} e^{K\sum_{j=1}^{5}[s_j(s_{j+6}+s_{j+7})+s_{j+6}s_{j+7}]} \times e^{K[s_6(s_7+s_{12})+s_7s_{12}]+K'\prod_{j=7}^{12}s_j} \prod_{i=1}^{6} u_n(s_i), \tag{A2}$$

where it is supposed that the corresponding star kagomelike recursive tree has n layers ($n \to \infty$) and $u_n(s_i)$, $i = 1, \dots, 6$ represent partition functions of six independent branches of the corresponding whole recursive tree with base sites with spin variables s_i (see Fig. 1). They have the following general form:

$$u_n(s_i) = \sum_{s_{i,1},\dots s_{i,11}} e^{K\sum_{j=1}^{5}[s_{i,j}(s_{i,j+5}+s_{i,j+6})+s_{i,j+5}s_{i,j+6}]} \times e^{K[s_i(s_{i,6}+s_{i,11})+s_{i,6}s_{i,11}]+K'\prod_{j=6}^{11}s_{i,j}} \prod_{j=1}^{5} u_{n-1}(s_{i,j}), \tag{A3}$$

where the sites of the layer $n-1$ of the recursive tree are numbered in the way as explicitly demonstrated in Fig. 1 for $i = 1$. Further, the explicit form of $u_n(s_i)$ for $s_i = -1$ and $s_i = +1$ [denoted as $u_n(-)$ and $u_n(+)$, respectively] is

$$\begin{aligned} u_n(-) = e^{-K'-6K}\{&[10e^{2K'} + 6e^{2(K'+6K)} + 6e^{2K'+4K} + 9e^{2K'+8K} + e^{2K'+24K} + 12e^{4K} + 6e^{8K} + 6e^{16K} + 8] \\ &\times u_{n-1}^5(-) + 5[7e^{2K'} + 2e^{2(K'+6K)} + e^{2(K'+8K)} + 9e^{2K'+4K} + 12e^{2K'+8K} + e^{2K'+20K} + 14e^{4K} + 4e^{8K} \\ &+ 6e^{12K} + 2e^{16K} + 6]u_{n-1}^4(-)u_{n-1}(+) + 2[25e^{2K'} + 14e^{2(K'+6K)} + 9e^{2(K'+8K)} + 62e^{2K'+4K} + 50e^{2K'+8K} \\ &+ 52e^{4K} + 50e^{8K} + 24e^{12K} + 4e^{16K} + 30]u_{n-1}^3(-)u_{n-1}^2(+) + 2[21e^{2K'} + 28e^{2(K'+6K)} + 3e^{2(K'+8K)} \\ &+ 72e^{2K'+4K} + 36e^{2K'+8K} + 42e^{4K} + 66e^{8K} + 18e^{12K} + 3e^{16K} + 31]u_{n-1}^2(-)u_{n-1}^3(+) \\ &+ [25e^{2K'} + 14e^{2(K'+6K)} + 9e^{2(K'+8K)} + 62e^{2K'+4K} + 50e^{2K'+8K} + 52e^{4K} + 50e^{8K} + 24e^{12K} + 4e^{16K} \\ &+ 30]u_{n-1}(-)u_{n-1}^4(+) + [7e^{2K'} + 2e^{2(K'+6K)} + e^{2(K'+8K)} + 9e^{2K'+4K} + 12e^{2K'+8K} + e^{2K'+20K} \\ &+ 14e^{4K} + 4e^{8K} + 6e^{12K} + 2e^{16K} + 6]u_{n-1}^5(+)\} \end{aligned} \tag{A4}$$

and

$$\begin{aligned} u_n(+) = e^{-K'-6K}\{&[7e^{2K'} + 2e^{2(K'+6K)} + e^{2(K'+8K)} + 9e^{2K'+4K} + 12e^{2K'+8K} + e^{2K'+20K} + 14e^{4K} + 4e^{8K} \\ &+ 6e^{12K} + 2e^{16K} + 6]u_{n-1}^5(-) + [25e^{2K'} + 14e^{2(K'+6K)} + 9e^{2(K'+8K)} + 62e^{2K'+4K} + 50e^{2K'+8K} + 52e^{4K} \end{aligned}$$

$$+50e^{8K}+24e^{12K}+4e^{16K}+30]u_{n-1}^4(-)u_{n-1}(+)+2[21e^{2K'}+28e^{2(K'+6K)}+3e^{2(K'+8K)}+72e^{2K'+4K}$$
$$+36e^{2K'+8K}+42e^{4K}+66e^{8K}+18e^{12K}+3e^{16K}+31]u_{n-1}^3(-)u_{n-1}^2(+)+2[25e^{2K'}+14e^{2(K'+6K)}$$
$$+9e^{2(K'+8K)}+62e^{2K'+4K}+50e^{2K'+8K}+52e^{4K}+50e^{8K}+24e^{12K}+4e^{16K}+30]u_{n-1}^2(-)u_{n-1}^3(+)$$
$$+5[7e^{2K'}+2e^{2(K'+6K)}+e^{2(K'+8K)}+9e^{2K'+4K}+12e^{2K'+8K}+e^{2K'+20K}+14e^{4K}+4e^{8K}+6e^{12K}$$
$$+2e^{16K}+6]u_{n-1}(-)u_{n-1}^4(+)+[10e^{2K'}+6e^{2(K'+6K)}+6e^{2K'+4K}+9e^{2K'+8K}+e^{2K'+24K}+12e^{4K}$$
$$+6e^{8K}+6e^{16K}+8]u_{n-1}^5(+)\}. \quad \text{(A5)}$$

Finally, the only independent recursion relation of the studied model given in Eq. (2) is defined as the ratio

$$x_n=\frac{u_n(+)}{u_n(-)}. \quad \text{(A6)}$$

[1] A. P. Ramirez, Annu. Rev. Matter. Sci. **24**, 453 (1994).
[2] J. E. Greedan, J. Mater. Chem. **11**, 37 (2001).
[3] J. S. Gardner, M. J. P. Gingras, and J. E. Greedan, Rev. Mod. Phys. **82**, 53 (2010).
[4] C. Lacroix, P. Mendels, and F. Mila (Eds.), *Introduction to Frustrated Magnetism*, Springer Series in Solid-State Sciences Vol. 164 (Springer-Verlag, Berlin, 2011).
[5] H. T. Diep (Ed.), *Frustrated Spin Systems* (World Scientific, Singapore, 2013).
[6] L. Savary and L. Balents, Rep. Prog. Phys. **80**, 016502 (2017).
[7] T. Lookman and X. Ren (Eds.), *Frustrated Materials and Ferroic Glasses* (Springer Nature, Switzerland, 2018).
[8] A. P. Ramirez, A. Hayashi, R. J. Cava, R. Siddharthan, and B. S. Shastry, Nature (Lond.) **399**, 333 (1999).
[9] K. Matsuhira, Z. Hiroi, T. Tayama, S. Takagi, and T. Sakakibara, J. Phys.: Condens. Matter **14**, L559 (2002).
[10] Z. Hiroi, K. Matsuhira, S. Takagi, T. Tayama, and T. Sakakibara, J. Phys. Soc. Jpn. **72**, 411 (2003).
[11] S. S. Sosin, L. A. Prozorova, A. I. Smirnov, A. I. Golov, I. B. Berkutov, O. A. Petrenko, G. Balakrishnan, and M. E. Zhitomirsky, Phys. Rev. B **71**, 094413 (2005).
[12] X. Ke, D. V. West, R. J. Cava, and P. Schiffer, Phys. Rev. B **80**, 144426 (2009).
[13] A. M. Hallas, A. M. Arevalo-Lopez, A. Z. Sharma, T. Munsie, J. P. Attfield, C. R. Wiebe, and G. M. Luke, Phys. Rev. B **91**, 104417 (2015).
[14] B. Wolf, U. Tutsch, S. Dörschung, C. Krellner, F. Ritter, W. Assmus, and M. Lang, J. Appl. Phys. **120**, 142112 (2016).
[15] S. Lucas, K. Grube, C.-H. Huang, A. Sakai, W. Wunderlich, E. L. Green, J. Wosnitza, V. Fritsch, P. Gegenwart, O. Stockert, and H. V. Löhneysen, Phys. Rev. Lett. **118**, 107204 (2017).
[16] M. Orendáč, P. Farkašovský, L. Regeciová, S. Gabáni, G. Pristáš, E. Gažo, J. Backai, P. Diko, A. Dukhnenko, N. Shitsevalova, K. Siemensmeyer, and K. Flachbart, Phys. Rev. B **102**, 174422 (2020).
[17] G. Toulouse, Commun. Phys. **2**, 115 (1977).
[18] M. J. Harris, S. T. Bramwell, D. F. McMorrow, T. Zeiske, and K. W. Godfrey, Phys. Rev. Lett. **79**, 2554 (1997).
[19] M. J. Harris, S. T. Bramwell, P. C. W. Holdsworth, and J. D. M. Champion, Phys. Rev. Lett. **81**, 4496 (1998).
[20] S. T. Bramwell and M. J. Harris, J. Phys.: Condens. Metter. **10**, L215 (1998).
[21] A. S. Wills, R. Ballou, and C. Lacroix, Phys. Rev. B **66**, 144407 (2002).
[22] R. Nath, A. A. Tsirlin, E. E. Kaul, M. Baenitz, N. Büttgen, C. Geibel, and H. Rosner, Phys. Rev. B **78**, 024418 (2008).
[23] E. Jurčišinová and M. Jurčišin, Physica A **486**, 296 (2017).
[24] J. L. Monroe, J. Stat. Phys. **65**, 255 (1991).
[25] J. L. Monroe, J. Stat. Phys. **67**, 1185 (1992).
[26] J. L. Monroe, Physica A **256**, 217 (1998).
[27] M. Pretti, J. Stat. Phys. **111**, 993 (2003).
[28] T. Yokota, Physica A **379**, 534 (2007).
[29] T. Yokota, Physica A **387**, 3495 (2008).
[30] E. Jurčišinová, M. Jurčišin, and A. Bobák, Phys. Lett. A **377**, 2712 (2013).
[31] E. Jurčišinová, M. Jurčišin, and A. Bobák, J. Stat. Phys. **154**, 1096 (2014).
[32] J. Strečka and C. Ekiz, Phys. Rev. E **91**, 052143 (2015).
[33] J. Strečka and C. Ekiz, Phys. Rev. E **102**, 012132 (2020).
[34] E. Jurčišinová and M. Jurčišin, Physica A **521**, 330 (2019).
[35] K. Kanô and S. Naya, Prog. Theor. Phys. **10**, 158 (1953).
[36] P. Azaria, H. T. Diep, and H. Giacomini, Phys. Rev. Lett. **59**, 1629 (1987).
[37] M. Debauche, H. T. Diep, P. Azaria, and H. Giacomini, Phys. Rev. B **44**, 2369 (1991).
[38] W. Li, S.-S. Gong, Y. Zhao, S.-J. Ran, S. Gao, and G. Su, Phys. Rev. B **82**, 134434 (2010).
[39] X. Yao, J. Magn. Magn. Mater. **322**, 959 (2010).
[40] Y. Zhao, W. Li, B. Xi, Z. Zhang, X. Yan, S.-J. Ran, T. Liu, and G. Su, Phys. Rev. E **87**, 032151 (2013).
[41] M. K. Ramazanov, A. K. Murtazaev, M. A. Magomedov, and M. K. Badiev, Phase Transitions **91**, 610 (2018).
[42] R. J. Baxter, *Exactly Solved Models in Statistical Mechanics* (Academic Press, London, 1982).
[43] P. D. Gujrati, Phys. Rev. Lett. **74**, 809 (1995).
[44] N. S. Ananikian, N. Sh. Izmailian, and K. A. Oganessyan, Physica A **254**, 207 (1998).
[45] E. Jurčišinová and M. Jurčišin, J. Stat. Phys. **147**, 1077 (2012).
[46] I. Syozi, Prog. Theor. Phys. **6**, 306 (1951).
[47] E. Jurčišinová and M. Jurčišin, Phys. Rev. E **97**, 052129 (2018).
[48] E. Jurčišinová and M. Jurčišin, Phys. Rev. E **99**, 042151 (2019).
[49] E. Jurčišinová and M. Jurčišin, J. Magn. Magn. Mater. **451**, 137 (2018).
[50] T. Amemiya, I. Umegaki, H. Tanaka, T. Ono, A. Matsuo, and K. Kindo, Phys. Rev. B **85**, 144409 (2012).